JOURNAL OF AGRICULTURAL AND FOOD CHEMISTRY
ARTICLE

J. Agric. Food Chem. 2010, 58, 9563–9571 9563
DOI:10.1021/jf100508j

Ganoderma lucidum Polysaccharides Attenuate Endotoxin-Induced Intercellular Cell Adhesion Molecule-1 Expression in Cultured Smooth Muscle Cells and in the Neointima in Mice

Ching-Yuang Lin,[†,#] Yung-Hsiang Chen,[‡,#] Chia-Ying Lin,[§,#] Hsien-Yeh Hsu,[∥] Shu-Huei Wang,[§] Chan-Jung Liang,[§] I-I Kuan,[§] Pei-Jhen Wu,[§] Pei-Ying Pai,[†] Chau-Chung Wu,*[,⊥] and Yuh-Lien Chen*[,§]

[†]Institute of Clinical Medical Science, and [‡]Graduate Institute of Integrated Medicine, China Medical University, Taichung, Taiwan, [§]Department of Anatomy and Cell Biology, National Taiwan University, Taipei, Taiwan, [∥]Faculty of Medical Technology, Institute of Biotechnology in Medicine, National Yang-Ming University, Taipei, Taiwan, and [⊥]Department of Internal Medicine and Primary Care Medicine, National Taiwan University Hospital, Taipei, Taiwan. [#]These authors contributed equally to the study

The expression of adhesion molecules on vessels and subsequent leukocyte recruitment are critical events in vascular diseases and inflammation. The aim of the present study was to examine the effects of an extract of *Ganoderma lucidum* (Reishi) polysaccharides (EORP), which is effective against cancer and immunological disorders, on adhesion molecule expression by human aortic smooth muscle cells (HASMCs) and the underlying mechanism. EORP significantly suppressed lipopolysaccharide (LPS)-induced intercellular cell adhesion molecule-1 (ICAM-1) mRNA and protein expression and reduced the binding of human monocytes to LPS-stimulated HASMCs. Immunoprecipitation and real-time polymerase chain reaction demonstrated that EORP markedly reduced the interaction of human antigen R protein (HuR) with the 3′-UTR of ICAM-1 mRNA in LPS-stimulated HASMCs. EORP treatment also suppressed extracellular signal-regulated kinase (ERK) phosphorylation and reduced the density of the shifted bands of nuclear factor (NF)-κB after LPS-induced activation. In an endothelial-denuded artery model in LPS-treated mice, daily oral administration of EORP for 2 weeks decreased neointimal hyperplasia and ICAM-1 expression in the plasma and neointima. These results provide evidence that EORP attenuates LPS-induced adhesion molecule expression and monocyte adherence and that this protective effect is mediated by decreased ERK phosphorylation and NF-κB activation. These findings suggest that EORP has anti-inflammatory properties and could prove useful in the prevention of vascular diseases and inflammatory responses.

KEYWORDS: *Ganoderma lucidum* polysaccharides; adhesion molecule; smooth muscle cells; MAPKs; vascular diseases

INTRODUCTION

The migration of vascular smooth muscle cells (VSMCs) into the intima and their subsequent proliferation, together with monocyte recruitment, after balloon injury and stent implantation play key roles in cardiovascular disorders. Many lines of evidence suggest that these events are preceded and accompanied by inflammation (*1*). The abnormal excessive expression of cell adhesion molecules, such as intercellular cell adhesion molecule-1 (ICAM-1), on VSMCs is responsible for the pathological changes in vascular and inflammatory diseases, such as atherosclerosis, restenosis, and transplant vasculopathy (*2*). Regulation of adhesion molecule expression is dependent on a complex array of intracellular signaling pathways involving RNA binding proteins, mitogen-activated protein kinases (MAPKs), and transcriptional factors (*3*, *4*). Recent studies have shown that certain drugs can eliminate the expression of adhesion molecules and signaling molecules, thereby attenuating the monocyte adhesion that leads to cardiovascular disorders (*5*).

Ganoderma lucidum (*G. lucidum*, Reishi), a popular home remedy, has long been known for its beneficial effects on human health and longevity and is used to treat chronic hepatopathy, hypertension, hyperglycemia, and neoplasia (*6*, *7*). Studies on the role of *G. lucidum* in regulating various body functions have revealed that *G. lucidum* polysaccharides are the bioactive constituents responsible for many of its health benefits, such as its antioxidant, anticancer, anti-inflammatory, and immunomodulatory activities (*8*−*11*). The effects of *G. lucidum* on the immune system have been linked to induction of cytokine expression and differentiation of macrophages (*12*, *13*) and the maturation of cultured murine bone marrow-derived dendritic cells (*14*).

*To whom correspondence should be addressed. Tel: +886-2-23123456-88176. Fax: +886-2-33931713. E-mail: ylchenv@ntu.edu.tw (Y.-L.C.) or chauchungwu@ntu.edu.tw (C.C.W.).

Published on Web 08/05/2010

G. lucidum polysaccharides inhibit inducible nitric oxide synthase expression in macrophages by its antioxidant properties (*15*) and exhibit antitumor activity and reduce tumor metastasis (*8*). A *G. lucidum* extract inhibited the proliferation of human prostate cancer cells (*16*) and had anticancer effects against HL-60 and U937 leukemic cell lines (*11*). Despite numerous studies, the function and the mechanism involved in these activities of *G. lucidum* polysaccharides have not been firmly demonstrated in cardiovascular disorders, characterized by monocyte adhesion and smooth muscle cells proliferation. In additional, little is known about the effects of an extract of Reishi polysaccharides (EORP) on adhesion molecule expression and the mechanisms of these effects, and a better understanding of this might provide important insights into the prevention of cardiovascular diseases and inflammation. We were therefore interested in understanding the mechanism of action of EORP on human aortic smooth muscle cells (HASMCs) stimulated by inflammatory cytokines and whether it affects the expression of adhesion molecules, an important event in vascular diseases and inflammation. In addition, we studied the effects of EORP on intimal thickening and ICAM-1 expression in the endothelial-denuded artery model in lipopolysaccharide (LPS)-treated mice. Our results showed that EORP attenuated ICAM-1 expression both in vitro and in vivo and that this effect was mediated, at least in part, through inhibition of human antigen R (HuR) translocation, extracellular signal-regulated kinase (ERK) phosphorylation, and nuclear factor (NF)-κB activation.

MATERIALS AND METHODS

Preparation of EORP. The biologically active compounds from *G. lucidum*, identified as the fucose-containing glycoprotein fraction and named EORPs, were isolated as described previously (*7*, *12*). A crude powder of *G. lucidum* prepared via alkaline extraction with 0.1 N NaOH, followed by neutralization and ethanol precipitation, was obtained from Pharmanex (Provo, UT). The crude powder of *G. lucidum* (6 g) was dissolved in 120 mL of double-distilled water, stirred at 4 °C for 12 h, and centrifuged at 250 g for 1 h at 4 °C to remove insoluble material. The resulting solution was concentrated at 40−50 °C to a small volume and lyophilized to generate 5 g of dark brown powder. This water-soluble residue was stored at −20 °C until used for further purification. Briefly, a 2.1 g sample was dissolved in a small volume of 0.1 M Tris buffer, pH 7.0, containing 0.1% sodium azide and purified by gel filtration chromatography at 4 °C using a Sephacryl S-500 column (95 cm × 2.6 cm), as the eluent at a flow rate of 0.6 mL/min and collecting 6.0 mL per tube. Each fraction was subjected to carbohydrate detection with phenol−H_2SO_4, and then, five fractions (fractions 1−5) were pooled, concentrated at 40−50 °C to a small volume, dialyzed to remove salts and sodium azide, and lyophilized to give 520 mg (25%) of EORP.

Culture of HASMCs. HASMCs, obtained as cryopreserved tertiary cultures from Cascade Biologics (Oregon), were grown in culture flasks in smooth muscle cell growth medium supplemented with 5% fetal bovine serum (FBS) at 37 °C in a humidified atmosphere of 95% air and 5% CO_2. The cells were passaged at 3−5 days (confluence) and were used between passages 3 and 8. Cultured cells were identified as smooth muscle cells on the basis of their morphology and the presence of smooth muscle-specific α-actin, as demonstrated by indirect immunofluorescence microscopy.

Effect of LPS and EORP on Cell Viability. HASMCs were plated at a density of 10^4 cells/well in 96-well plates. After overnight growth, the cells were treated with different concentrations of LPS or EORP, and then, cell viability was measured using the 3-(4,5-dimethylthiazol-2-yl)-2,5-diphenyltetrazolium bromide (MTT) assay.

Testing of the Effect of Preincubation with EORP on the Effects of LPS. HASMCs (10^6 cells in 5 mL of medium in a 10 cm Petri dish) were incubated with the indicated concentration of EORP or medium for the indicated time, then medium or the indicated concentration of LPS was added, and incubation continued for the indicated time.

Preparation of Cell Lysates and Nuclear and Cytosolic Fractions. To prepare cell lysates, the cells were lysed for 1 h at 4 °C in 20 mM Tris-HCl, 150 mM NaCl, 1 mM EDTA, 1 mM EGTA, 1% Triton X-100, and 1 mM phenylmethylsulfonyl fluoride (PMSF), pH 7.4, then the lysate was centrifuged at 4000*g* for 30 min at 4 °C, and the supernatant was retained.

To prepare nuclear and cytosolic proteins, the cells were washed with PBS, pelleted, and lysed on ice for 15 min in 0.1 mM EDTA, 10 mM HEPES, 10 mM KCl, 0.1 mM EGTA, 1 mM DTT, 0.5 mM PMSF, 1 mM NaF, 1 mM Na_3VO_4, and 0.6% NP-40, then the lysates were centrifuged at 12000*g* at 4 °C for 10 min, and the resulting nuclear pellet and supernatant (cytosolic fraction) were stored at −80 °C for Western blot analysis.

Western Blot Analysis. Western blot analyses were performed as described previously (*17*). An aliquot of sample (20 μg of total protein) was subjected to 12% sodium dodecyl sulfate−polyacrylamide gel electrophoresis (SDS-PAGE) electrophoresis and transferred to PVDF membranes, which were then blocked for 1 h at room temperature with 1% bovine serum albumin (BSA) in PBS−0.05% Tween 20.

To measure ICAM-1 or VCAM-1 levels, the membranes were incubated with goat antihuman ICAM-1 or with VCAM-1 antibodies (1:1000 dilution in 5% BSA in PBS, R&D Systems, MN) and then with horseradish peroxidase (HRP)-conjugated mouse antigoat IgG antibodies (1:3000 dilution in 5% BSA in PBS, R&D Systems), bound antibody being detected using Chemiluminescence Reagent Plus (NEN). The intensity of each band was quantified using a densitometer. Anti-β-actin antibodies (1:10000, Oncogen) were used to quantify β-actin, used as the internal control.

In other studies, the antibodies used were mouse antihuman HuR or antihuman heterogeneous nuclear ribnucleoproteins (hnRNP) (Abcam), rabbit antihuman phospho-Jun N-treminal kinase (JNK), mouse antihuman phopho-ERK1/2, rabbit antihuman phospho-p38, rabbit antihuman total JNK, rabbit antihuman total ERK1/2, goat antihuman total p38 (all 1:1000, Cell Signaling), and rabbit antihuman IκBα (1:5000, Santa Cruz) followed by HRP-conjugated goat antirabbit IgG antibodies (1:3000, Sigma) or goat antimouse IgG or rabbit antigoat IgG antibodies (1: 3000, both from Chemicon), as appropriate.

Quantitative Real-Time Polymerase Chain Reaction (RT-PCR). Total RNA was isolated using a TRIZOL reagent kit (Invitrogen, CA), and quantitative RT-PCR was performed using a Brilliant II SYBR Green QRT-PCR master mix kit (Stratagene, CA). Each reaction mixture (25 μL final volume) contained 12.5 μL of 2X SYBR QRT-PCR master mix, upstream and downstream primers (100 nM), 0.375 μL of reference dye, and 1 μL of StrataScript RT/RNase block enzyme mixture. Real-time fluorescence monitoring and melting curve analysis were performed using a Stratagene Mx3000P RT-PCR system. The ICAM-1-specific oligonucleotide primer pair consisted of the forward primer 5′-CCG GAA GGT GTA TGA ACT G-3′ and the reverse primer 5′-TCC ATG GTG ATC TCT CCT C-3′. The β-actin as the control was carried out using the forward and reverse primers 5′-CTG GAC TTC GAG CAA GAG ATG-3′ and 5′-TGA TGG AGT TGA AGG TAG TTT CG-3′. The PCR conditions were 50 °C for 60 min, 95 °C for 10 min, and 40 cycles of 95 °C for 30 s, 60 °C for 30 s, and 68 °C for 60 s. Data were analyzed using Stratagene MxPro-Mx3000P QPCR software version 3.00 (Stratagene). RT-PCR was monitored by measuring the fluorescent signal at the end of the annealing phase for each cycle. ICAM-1 mRNA levels were normalized to β-actin mRNA levels.

Cross-Linking Immunoprecipitation Assay for the RNA−Protein Interaction. To determine whether HuR interacted directly with the 3′-UTR of ICAM-1 mRNA, immunoprecipitation and RT-PCR were carried out. To induce cross-linking, cells in ice-cold PBS were irradiated three times with 4000 mJ of ultraviolet-B light at intervals of 3 min. The cells were then lysed with cold cell lysis buffer (10 mM HEPES, 10 mM KCl, 0.1 mM EGTA, 0.1 mM EDTA, 1 mM DTT, 0.5 mM PMSF, 1 mM NaF, 1 mM Na_3VO_4, and 0.6% NP-40), the cytoplasmic fraction was prepared by centrifugation (1400*g*, 4 °C, 5 min), and then, aliquots (500 μg of protein) were incubated with 10 μg of anti-HuR antibody (Santa Cruz) and Protein G-Sepharose (GE Healthcare) for 1 h at 4 °C. The RNA in the immunoprecipitated material was then extracted using TRIZOL reagent and used in a quantitative RT-PCR reaction to detect the presence of the 3′-UTR of ICAM-1 mRNA. The mRNA was reverse-transcribed using a Reverse-iT first Strand Synthesis Kit (AB gene, United States), and then, quantitative RT-PCR was used to measure the 3′-UTR transcript levels. The PCR primers used for the 3′-UTR of ICAM-1 mRNA were 5′-CCA TCG ATG CCT GCT GGA TGA GAC TCC TGC-3′ and 5′-CCA TCG ATA GAC TCT CAC AGC ATC TGC AGC-3′.

Smooth Muscle Cell-Leukocyte Adhesion Assay. HASMCs (5×10^5) were plated in the wells of 24-well plates and allowed to reach confluence. They were then incubated for 24 h at 37 °C with growth medium supplemented with 0.25 μg/mL of EORP and then for 24 h at 37 °C with growth medium containing 0.1 μg/mL of LPS in the continued presence of EORP. U937 cells, originally derived from a human histiocytic lymphoma and obtained from the American Type Culture Collection (Rockville, MD), were labeled for 1 h at 37 °C with 10 μM BCECF/AM (Boehringer-Mannheim) in serum-free RPMI 1640 medium.

Labeled U937 cells (10^6) were added to each HASMC-containing well, and incubation continued for 1 h. Nonadherent cells were removed by two gentle washes with PBS, and then, the number of bound U937 cells was determined by counting four different fields using a fluorescence microscope at 400× magnification. Fields for counting adherent cells were randomly selected at a half-radius distance from the center of the monolayer.

Knockdown of Gene Expression Using Small Interfering RNA. Knockdown of ERK gene expression was performed by transfection with small interfering RNA (siRNA). HASMCs (10^6) were resuspended in 100 μL of Nucleofector solution (Amaxa Biosystems, Germany), and gene-specific siRNA oligomers (1 μM) were electroporated according to the manufacturer's instruction manual. The ERK siRNAs (catalog nos. 10620319 124945 F11 and 10620318 124945 F12, Invitrogen) were AUA UUC UGU CAG GAA CCC UGU GUG A and UCA CAC AGG GUU CCU GAC AGA AUA U. The Stealth RNAi Negative Control Med GC that has no homology to the vertebrate transcriptome was used as the negative control (siCL).

Nuclear Extract Preparation and Electrophoretic Mobility Shift Assay (EMSA). The preparation of nuclear extracts and the conditions for the EMSA have been described previously (*17*). The 22-mer synthetic double-stranded oligonucleotides used as the NF-κB and activator protein (AP-1) probes in the gel shift assay were, respectively, 5′-AGT TGA GGG GAC TTT CCC AGG C-3′ and 3′-TCA ACT CCC CTG AAA GGG TCC G-5′ and 5′-ATT CGA TCG GGG CGG GGC GAG C-3′ and 3′-TAA GCT AGC CCC GCC CCG CTC G-5′.

Mouse Femoral Arterial Injury Model and Immunohistochemical Staining. All procedures involving experimental animals were performed in accordance with the guidelines for animal care of the National Taiwan University and complied with the "Guide for the Care and Use of Laboratory Animals" NIH publication No. 86-23, revised 1985. Male 8 week old C57BL6 mice ($n = 48$), weighing between 25 and 35 g, were anesthetized by intraperitoneal (ip) injection of 30−40 mg/kg of pentobarbital. *trans*-Luminal mechanical injury of the left femoral artery was induced basically according to the method developed by Sata et al. (*18*). To examine the effects of EORP administration on neointimal formation in the endothelial-denuded femoral artery, the mice were divided into four groups. The treatment period was 2 weeks (days 0−14), with D1 being the day of endothelial denudation. Groups 1 and 2 were given, respectively, either PBS or 1 mg/kg/day of LPS on days 1−14 by ip injection, and group 3 was treated with LPS in the same way as group 2 but received oral EORP at 60 mg/kg/day on days 0−14, and group 4 received only the oral EORP. The selection of EORP dose was based on its antitumor activity (*8*, *9*). At the end of treatment, blood samples were collected, and soluble ICAM-1 in the plasma was measured by enzyme-linked immunosorbent assay (ELISA) according to the manufacturer's instructions (R&D Systems). To examine expression of ICAM-1 protein on smooth muscle cells, immunohistochemistry was performed on serial sections of the femoral artery. The sections were incubated for 1 h at 37 °C with goat antihuman ICAM-1 or α-actin antibody (1:15 dilution in PBS, R&D Systems, Inc.) and for 1 h at room temperature with HRP rabbit antigoat IgG antibody (Sigma), bound antibody being detected by incubation for 1.5 h at room temperature with avidin−biotin−HRP complex, followed by 0.5 mg/mL of 3,3′-diaminobenzidine/0.01% hydrogen peroxide in 0.1 M Tris-HCl buffer, pH 7.2, as chromogen (Vector Lab, United States). Negative controls were performed by omitting the primary antibodies.

Statistical Analysis. Values are expressed as the mean ± standard error of the mean (SEM). Analysis of the variance was performed for statistical analysis. A P value < 0.05 was considered statistically significant.

RESULTS

EORP Reduces ICAM-1 mRNA and Protein Expression in LPS-Treated HASMCs. Cell viability was assessed using the MTT assay. Treatment of HASMCs with 0.025, 0.1, 0.5, or 1 μg/mL of LPS for 24 h did not result in cytotoxicity (data not shown). After 24 h of incubation with 0.25, 0.5, 1, 5, or 10 μg/mL of EORP, cell viability was, respectively, 100 ± 5, 95 ± 5, 76 ± 4, 68 ± 4, or 69 ± 3% of control levels, the three highest concentrations causing a significant reduction in cell viability.

To determine whether LPS alone or together with EORP affected levels of ICAM-1 protein, Western blotting was performed. LPS treatment induced ICAM-1 protein expression in a time- and dose-dependent manner (**Figure 1A**,**B**). As shown in **Figure 1C**, after treatment of the cells with 0.1 μg/mL of LPS for 24 h, ICAM-1 expression was increased about 3-fold, and this effect was significantly attenuated by 24 h pretreatment with 0.25 or 0.5 μg/mL of EORP (85 and 94% inhibition, respectively). The concentrations of 0.1 μg/mL of LPS and 0.25 μg/mL EORP were therefore used in subsequent experiments. The effect of EORP on ICAM-1 expression was also studied by immunofluorescent staining (**Figure 1D**). In untreated cells, ICAM-1 expression was weak, while in cells treated for 24 h with LPS, ICAM-1 expression was strong, and this effect was inhibited by pretreatment with EORP. Nevertheless, LPS did not induce VCAM-1, and EORP did not affect the result in HASMCs demonstrated by Western blot and immunofluorescent staining (**Figure 1E**,**F**).

To determine whether changes in ICAM-1 protein levels were associated with modification of ICAM-1 mRNA levels, quantitative RT-PCR was performed. As shown in **Figure 1G**, unstimulated HASMCs contained low amounts of ICAM-1 mRNA, and 4 h of treatment with LPS resulted in a marked increase in levels, which was markedly inhibited by preincubation with 0.25 μg/mL of EORP for 24 h (80% inhibition). In cells incubated with EORP alone, ICAM-1 mRNA levels were similar to those in unstimulated samples. Furthermore, the addition of 20 μg/mL of actinomycin D (a RNA polymerase inhibitor) or cycloheximide (a protein synthesis inhibitor) for 1 h before incubation with LPS for 4 h significantly reduced ICAM-1 mRNA levels in HASMCs, showing that LPS-induced ICAM-1 expression required de novo RNA and protein synthesis.

EORP Reduces LPS-Induced ICAM-1 Expression by Inhibiting HuR Translocation and the HuR−ICAM-1 mRNA Interaction. HuR is an ubiquitous RNA binding protein that is located predominantly in the nucleus in the unstimulated cell and is translocated to the cytoplasm in the stimulated cell (*19*). We investigated whether EORP pretreatment affected the subcellular distribution of HuR in LPS-treated HASMCs. As shown in **Figure 2A**, in nontreated HASMCs, HuR was found predominantly in the nucleus. Treatment with LPS caused a marked accumulation of HuR in the cytoplasm, and pretreatment with EORP resulted in a significant decrease in cytoplasmic HuR levels in LPS-treated HASMCs. To confirm the immunocytochemical staining results, Western blotting was performed to measure nuclear and cytoplasmic levels of HuR in HASMCs following treatment with LPS either alone or with EORP pretreatment. As shown in **Figure 2B**, LPS caused a marked increase in cytoplasmic levels of HuR without a concomitant decrease in nuclear HuR levels, and EORP markedly inhibited the accumulation of cytoplasmic HuR in LPS-treated HASMCs. On the basis of the cytoplasmic localization of HuR in LPS-treated HASMCs and the region of the AU-rich element (ARE) recognized by HuR, we postulated that HuR might interact with the 3′-UTR of ICAM-1 mRNA and assessed this possibility using immunoprecipitation with specific anti-HuR antibody and Protein G-Sepharose, followed by RT-PCR to estimate the amount of 3′-UTR of ICAM-1 mRNA in the immunoprecipitate. The mouse IgG was subjected to protein fractions of each group and was used as negative controls. As shown in **Figure 2C**, treatment with LPS for 4 h markedly increased the interaction of HuR with the

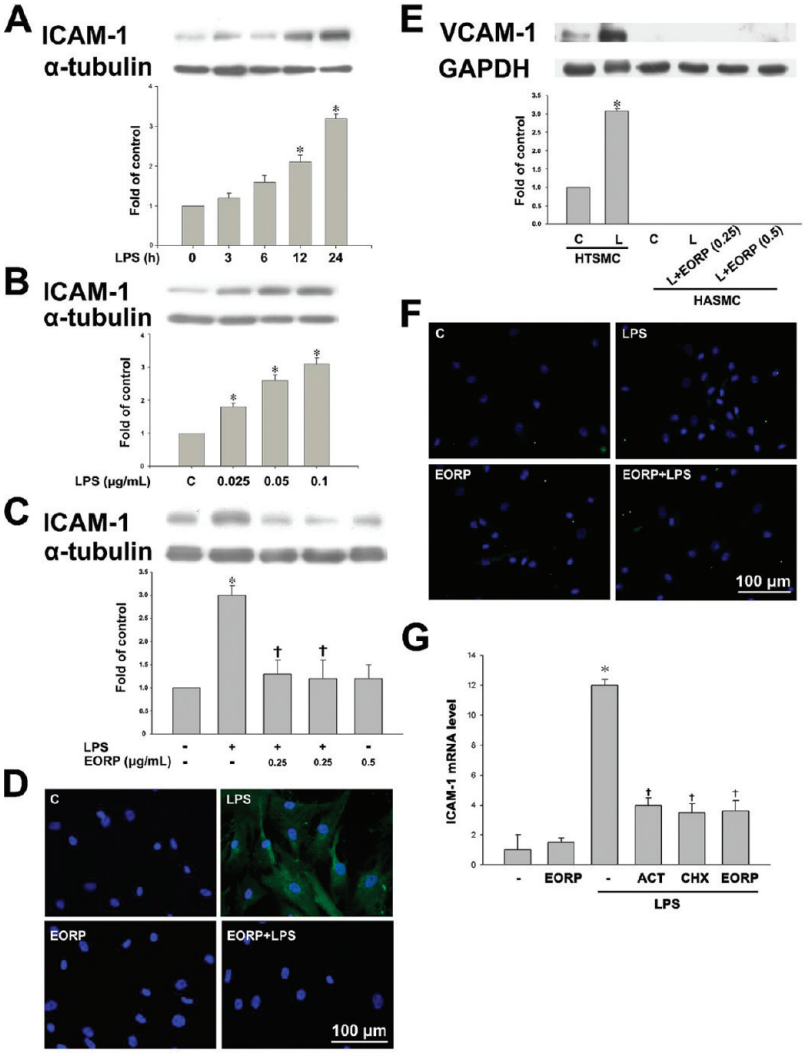

Figure 1. EORP reduces ICAM-1 mRNA and protein expression in LPS-treated HASMCs. (**A** and **B**) HASMCs were treated with 0.1 μg/mL of LPS for the indicated time (**A**) or with the indicated concentration of LPS for 24 h (**B**). (**C**) HASMCs were incubated for 24 h with 0, 0.25, or 0.5 μg/mL of EORP and then for 24 h with 0.1 μg/mL of LPS in the continued presence of the same concentration of EORP, and then, ICAM-1 expression was measured in cell lysates by Western blotting. α-Tubulin was used as the loading control. (**D**) The cells were treated as in panel **C**, and then, the distribution of ICAM-1 was analyzed by immunofluorescent microscopy. ICAM-1 expression is indicated by green fluorescence (FITC) and nuclei by blue fluorescence (DAPI). Bar = 100 μm. (**E**) HASMCs were incubated for 24 h with 0, 0.25, or 0.5 μg/mL of EORP and then for 24 h with 0.1 μg/mL of LPS in the continued presence of the same concentration of EORP, and then, VCAM-1 expression was measured in cell lysates by Western blotting. GAPDH was used as the loading control. The VCAM-1 expression of LPS-treated human tracheal smooth muscle cells (HTSMC) was used as the positive control. (**F**) The cells were treated as in panel **E**, and then, the distribution of VCAM-1 was analyzed by immunofluorescent microscopy. VCAM-1 expression is indicated by green fluorescence (FITC) and nuclei by blue fluorescence (DAPI). (**G**) Analysis of ICAM-1 mRNA levels in untreated HASMCs or HASMCs preincubated for 1 h with actinomycin D (ACT, 20 μg/mL), cycloheximide (CHX, 20 μg/mL), or EORP (0.25 μg/mL) and then incubated for 4 h with 0.1 μg/mL of LPS in the continued presence of the inhibitor. Total RNA was analyzed by quantitative RT-PCR after normalization to β-actin mRNA levels. In panels **A**, **B**, **C**, **E**, and **G**, the data are expressed as a fold value compared to the control value and are the means $\pm$ SEMs for three separate experiments. $^*P < 0.05$ as compared to the untreated cells. $^\dagger P < 0.05$ as compared to the LPS-treated cells.

3′-UTR of ICAM-1 mRNA, and this effect was markedly reduced by 24 h of preincubation with 0.25 μg/mL of EORP.

The EORP-Induced Reduction in LPS-Induced ICAM-1 Expression Is Dependent on the Inhibition of Phosphorylation of ERK. A previous study showed that LPS can activate MAPKs in the signaling pathway leading to inflammation (*20*). In the next set of experiments, the effects of LPS on the activation of the MAPK pathway (ERK1/2, JNK, and p38), a signaling cascade contributing to ICAM-1 expression, and the effects of MAPK inhibitors or siERK on LPS-stimulated ICAM-1 expression were studied. As shown in **Figure 3A**−**C**, phosphorylation of ERK, JNK, and p38 was, respectively, increased 5.6-, 3.0-, and 4.0-fold as compared to control levels 15 min after addition of LPS. Pretreatment for 24 h with 0.25 μg/mL of EORP decreased LPS-induced ERK phosphorylation but not JNK or p38 phosphorylation.

As shown in **Figure 3D**, the increase in ICAM-1 expression in response to LPS treatment was inhibited by 1 h of pretreatment with 30 μM PD98059 (an ERK1/2 inhibitor), while SP600125 (a JNK inhibitor) or SB203580 (a p38 inhibitor) had no effect. Interestingly, ICAM-1 expression was inhibited by transfection of HASMCs with ERK1/2-specific siRNA (1 μM) (**Figure 3E**). The effectiveness of the siRNA treatment was validated by showing that ERK1/2-specific siRNA (as compared to control siRNA) caused a 55% reduction in ERK1/2 protein expression (**Figure 3F**). These results suggest that EORP inhibits

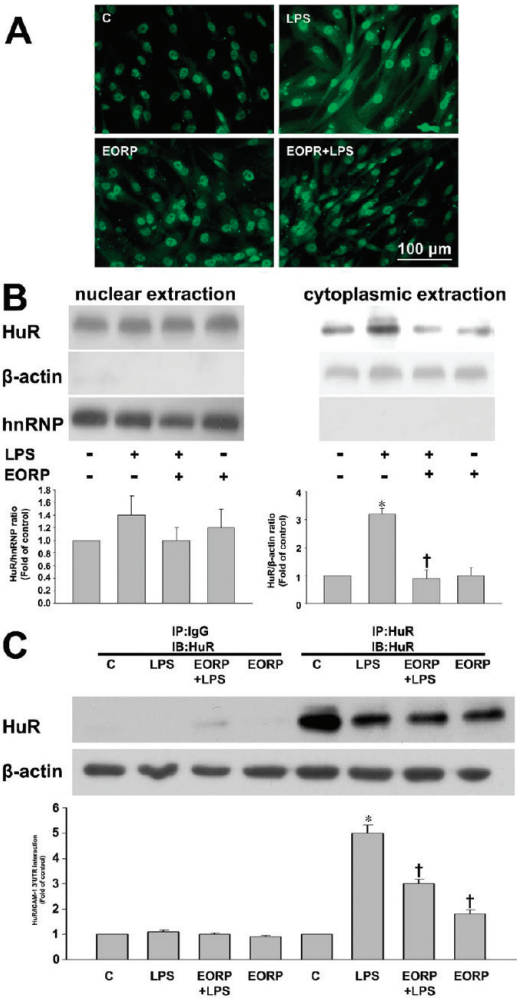

Figure 2. EORP-mediated reduction in LPS-induced ICAM-1 expression involves inhibition of HuR translocation and the HuR−ICAM-1 mRNA interaction. HASMCs were incubated for 24 h with EORP (0.25 μg/mL) and then with 0.1 μg/mL of LPS for 24 h in the continued presence of the same concentration of EORP, and HuR expression was measured by immunofluorescent staining and Western blotting. (**A**) Subcellular distribution of HuR in HASMCs shown by immunofluorescent microscopy. (**B**) Western blots showing HuR protein levels in the HASMC cytoplasm and nucleus. β-Actin and heterogeneous nuclear ribonucleoproteins (hnRNP) C1 and C2 were used as loading controls and to ensure lack of cross-contamination of the fractions. (**C**) The cytoplasmic fractions were subjected to immunoprecipitation using anti-HuR antiserum or nonimmune IgG. Proteins were resolved by SDS-PAGE and detected by Western blotting. Five microliters of immunoprecipitated material was used in quantitative RT-PCR reactions to detect the presence of the 3′-UTR of ICAM-1 mRNA. For immunoprecipitation experiments, an irrelevant isotype-matched IgG has been used as a negative control. In panels **B** and **C**, the data are presented as the means ± SEMs and represent the results from three independent experiments. $^{*}P < 0.05$ as compared to the unstimulated group. $^{\dagger}P < 0.05$ as compared to the LPS-treated cells.

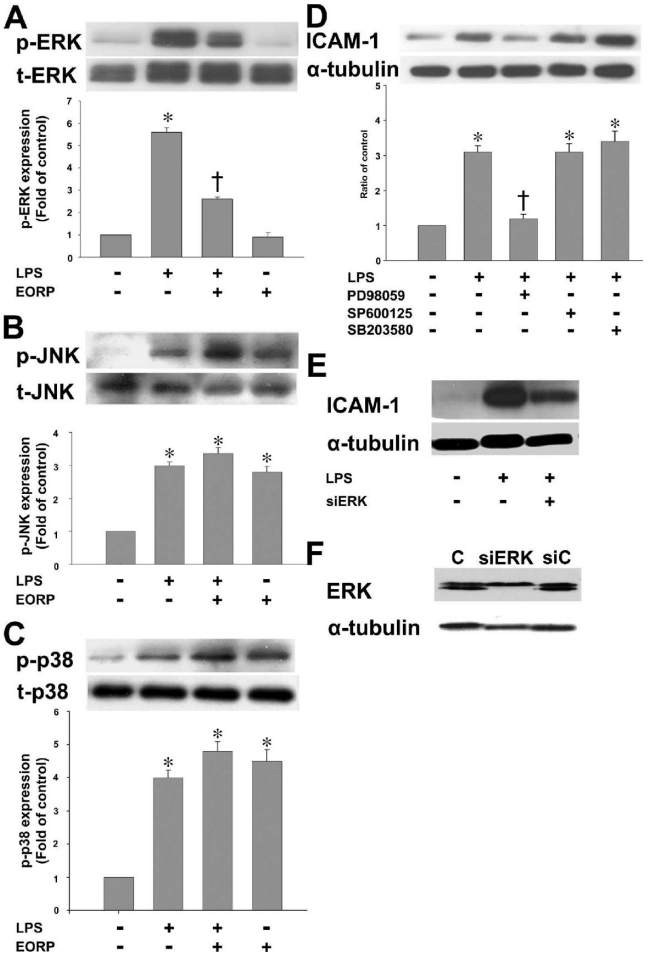

Figure 3. EORP-mediated reduction in LPS-induced ICAM-1 expression is dependent on inhibition of phosphorylation of ERK. (**A**−**C**) Western blot analysis showing the effect of EORP pretreatment on the phosphorylation of (**A**) ERK1/2, (**B**) JNK, or (**C**) p38 in LPS-treated HASMCs. HASMCs were incubated for 24 h with or without 0.25 μg/mL of EORP, and then, the cells were incubated with 0.1 μg/mL of LPS in the continued presence of the inhibitor for 15 min and aliquots of cell lysate containing equal amounts of protein subjected to immunoblotting with the indicated antibodies. (**D**) Effect of inhibitors of MAPK phosphorylation on ICAM-1 expression in control and LPS-treated HASMCs. HASMCs were incubated for 1 h with 30 μM PD98059 (an ERK1/2 inhibitor), SP600125 (a JNK inhibitor), or SB203580 (a p38 inhibitor) and then for 24 h with or without 0.1 μg/mL of LPS in the continued presence of the inhibitor, and then, ICAM-1 expression was measured by Western blotting. (**E**) The LPS-induced increase in ICAM-1 expression is inhibited by transfection of HAECs with ERK1/2-specific siRNA (1 μM). HASMCs were transfected with either control siRNA or ERK1/2-specific siRNA (1 μM) for 48 h, then were incubated with 0.25 μg/mL of EORP for 24 h, and then with 0.1 μg/mL of LPS for 24 h in the continued presence of the same concentration of EORP, and ICAM-1 expression was measured in cell lysates by Western blotting. (**F**) ERK1/2-specific siRNA (as compared to control siRNA; siC) causes a 55% reduction in ERK1/2 protein expression. HASMCs were transfected with either control or ERK1/2-specific siRNA (1 μM) for 48 h, and then, ERK expression was measured in cell lysates by Western blotting. In panels **A**−**D**, the data are expressed as a fold of the control value and are the means ± SEMs for three separate experiments. Total ERK (t-ERK), total p38 (t-p38), total JNK (t-JNK), or α-tubulin was used as the loading control for panels **A**, **B**, **C**, or **D**, respectively. $^{*}P < 0.05$ as compared to the untreated cells. $^{\dagger}P < 0.05$ as compared to the LPS-treated cells.

LPS-induced ICAM-1 expression by preventing LPS-induced phosphorylation of ERK.

EORP AttenUates Activation of NF-κB Expression and Nuclear Translocation of NF-κB p50 in LPS-Stimulated HASMCs. Transcriptional regulation involving NF-κB and AP-1 activation has been implicated in the cytokine-induced expression of adhesion molecules (*20*). As shown by Western blots (**Figure 4A**), the stimulatory effect of LPS on ICAM-1 levels was blocked by coincubation with parthenolide, an NF-κB inhibitor, but not by

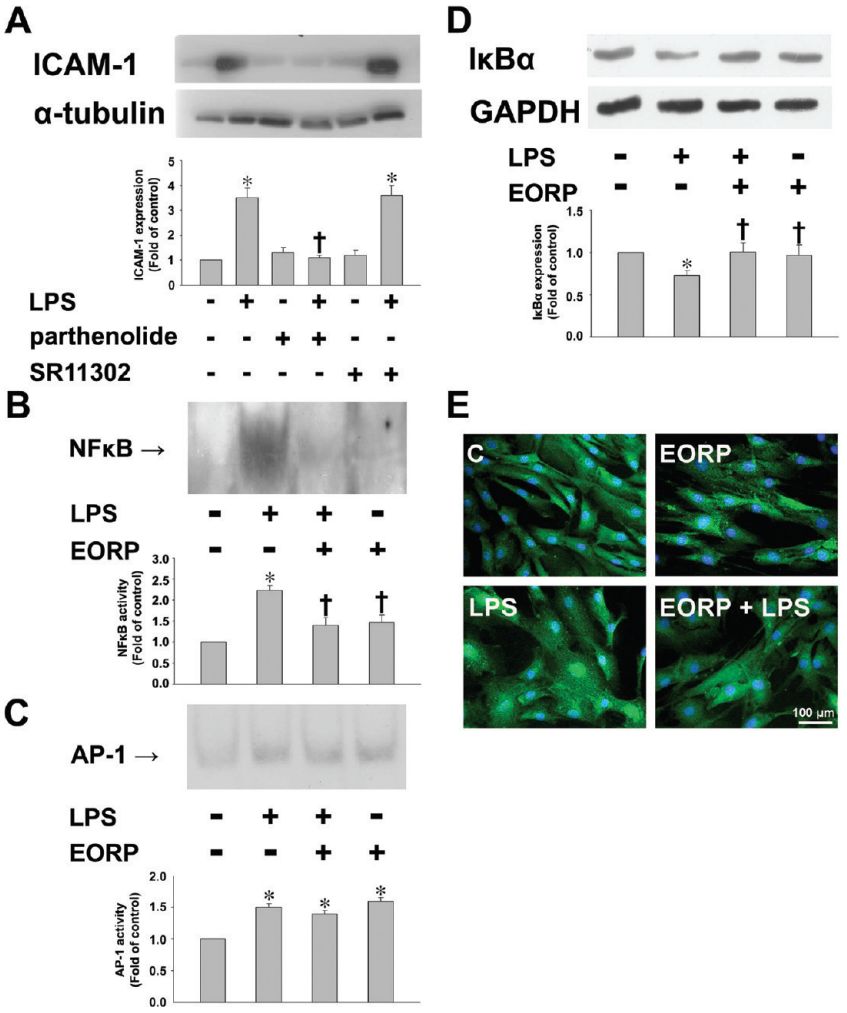

Figure 4. EORP-induced reduction in the upregulation of ICAM-1 expression in LPS-treated HASMCs is mediated by inhibition of both NF-κB activation and NF-κB p50 nuclear translocation. (**A**) Cells were coincubated for 24 h with 30 μM parthenolide (NF-κB inhibitor) or 30 μM SR11302 (AP-1 inhibitor) and 0.1 μg/mL of LPS, and then, cell lysates were prepared and assayed for ICAM-1 on Western blots. (**B** and **C**) Nuclear extracts prepared from untreated cells or from cells with or without EORP pretreatment (0.25 μg/mL, 24 h) and then incubated with 0.1 μg/mL of LPS for 30 min in the continued presence of the inhibitor were tested for NF-κB (**B**) or AP-1 (**C**) DNA binding activity by EMSA. (**D**) Western blotting of cytoplasmic proteins with IκBα antibodies. (**E**) Immunofluorescent staining for NF-κB p50. HASMCs were left untreated or incubated for 24 h with or without 0.25 μg/mL EORP and then with or without 0.1 μg/mL of LPS for 24 h in the continued presence of the EORP. NF-κB p50 expression is indicated by green fluorescence (FITC) and nuclei by blue fluorescence (DAPI). A representative result from three separate experiments is shown. Bar = 100 μm. $^*P < 0.05$ as compared to the untreated cells, $^\dagger P < 0.05$ as compared to the LPS-treated cells.

coincubation with SR11302, an activator protein-1 (AP-1) inhibitor. As shown in **Figure 4B**,**C**, low basal levels of NF-κB and AP-1 binding activity were detected in control cells, and binding was significantly increased by 30 min of treatment with LPS. The increased binding caused by LPS was blocked by a 100-fold excess of unlabeled AP-1 or NF-κB probe (data not shown). LPS-induced NF-κB binding activity was effectively reduced by 24 h of pretreatment with EORP, while AP-1 binding activity was not affected. In EORP-pretreated HASMCs, the LPS-induced increase in NF-κB binding was reduced by 40%. Western blot was also conducted to determine whether the activation of NF-κB in LPS-treated cells occurs by the proteolytic degradation of IκBα. LPS treatment caused degradation of IκBα, while EORP pretreatment decreased the degradation (**Figure 4D**). To determine whether NF-κB activation was involved in the pretranslational effects of EORP on adhesion molecule expression, we also studied NF-κB p50 expression in the nuclei of LPS-treated HASMCs by immunofluorescent staining. As shown in **Figure 4E**, LPS-stimulated HASMCs showed marked NF-κB p50 staining in the nuclei, while EORP-pretreated LPS-stimulated cells showed weaker nuclear NF-κB staining but stronger cytoplasmic staining.

EORP Inhibits the Adhesion of U937 Cells to LPS-Stimulated HASMCs. To explore the effects of EORP on the smooth muscle cell−leukocyte interaction, we examined the adhesion of U937 cells to LPS-treated HASMCs. As shown in **Figure 5**, control confluent HASMCs incubated with U937 cells for 1 h showed minimal binding, but adhesion was substantially increased when the HASMCs were pretreated with LPS for 24 h. Pretreatment of HASMCs for 24 h with 0.25 μg/mL of EORP reduced the number of U937 cells adherent to LPS-stimulated HASMCs by 90%. The involvement of ICAM-1 in the adhesion of U937 cells to LPS-treated HASMCs was examined by 24 h of pretreatment of the cells with 2 μg/mL of anti-ICAM-1 antibody before incubation with LPS, which resulted in significantly lower binding of U937 cells to HASMCs than in nonantibody-treated LPS-stimulated cells, showing that ICAM-1 plays a major role in the adhesion of U937 cells to LPS-treated HASMCs. The adherence of U937 cells to LPS-treated HASMCs was also inhibited by 30 μM PD98059 or

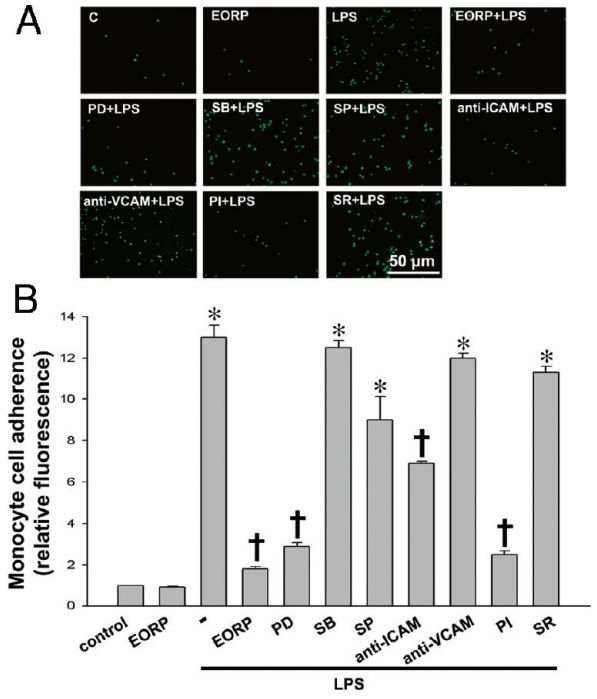

Figure 5. EORP reduces the adhesion of U937 cells to LPS-treated HASMCs. HASMCs were left untreated or were pretreated for 24 h with 0.25 μg/mL EORP or 30 μM PD98059 (PD), SB203580 (SB), SP600125 (SP), parthenolide (PI), or SR11302 (SR), 2 μg/mL of purified anti-ICAM-1 antibody, or 2 μg/mL of purified anti-VCAM-1 antibody and then with 0.1 μg/mL of LPS for 24 h in the continued presence of the inhibitor. (**A**) Representative fluorescent photomicrographs showing the effect on macrophage adhesion to HASMCs. C is untreated cells. Bar = 50 μm. (**B**) Fluorescence intensity of the bound monocytes expressed relative to that of the control cells. $^*P < 0.05$ as compared to untreated cells. $^\dagger P < 0.05$ as compared to LPS-treated cells.

parthenolide but not by anti-VCAM-1 antibody, SP600125, SB203580, or SR11302.

EORP Decreases ICAM-1 Expression in the Endothelial-Denuded Artery of LPS-Treated Mice. To examine the effects of EORP administration on neointimal formation in the endothelial-denuded femoral artery model, mice were divided into four groups. The treatment period was 2 weeks (days 0−14), with D1 being the day of endothelial denudation. Groups 1 and 2 were injected ip with PBS or 1 mg/kg/day of LPS, respectively, on days 1−14, group 3 was treated with LPS in the same way as group 2 but received oral EORP at 60 mg/kg/day on days 0−14, and group 4 received only the oral EORP. Over the experimental period, there was no difference in weight gain and final weight between the four groups. To detect the effect of LPS and EORP on ICAM-1 expression, we initially used an ELISA to quantify ICAM-1 levels in the plasma. As shown in **Figure 6A**, the endothelial-denuded artery mice produced 398 ± 10 ng/mL of ICAM-1 at 2 weeks, and this was little affected by oral EORP alone. In the LPS-treated mice, the concentration of ICAM-1 in the plasma increased, reaching 740 ± 70 ng/mL at 2 weeks. When LPS-treated mice were treated with 60 mg/kg/day of EORP for 2 weeks, only low levels of ICAM-1 were released.

Morphometric analysis showed that the intima/media area ratio in the EORP-treated LPS-treated endothelial-denuded mice (0.40 ± 0.10%, $n = 12$) was significantly lower than that in the LPS-treated endothelial-denuded mice (0.81 ± 0.21%, $n = 12$) (**Figure 6B**). To study the effect of EORP on ICAM-1 expression in LPS-treated mice, immunohistochemical staining with antibodies against ICAM-1 or anti-α-actin antibody (staining smooth muscle cells) was carried out on serial sections. In the LPS-treated mice, α-actin-positive staining was seen on the thickened intima of the femoral artery (lower panels in **Figure 6C**) and strong ICAM-1 staining was seen (upper panels). In contrast, in the EORP-treated, LPS-treated, endothelial-denuded artery, the intimal area was reduced and showed weaker ICAM-1 staining.

DISCUSSION

Herein, we demonstrated that EORP treatment effectively blocked ICAM-1 expression both in vitro in LPS-stimulated HASMCs and in vivo in the endothelial-denuded artery of LPS-treated mice. EORP decreased ICAM-1 expression and the binding of the human monocytic cell line U937 to LPS-treated HASMCs, and these effects might be mediated through inhibition of ERK phosphorylation and NF-κB activation. EORP attenuated the LPS-induced increase in both the HuR interaction with the 3′-UTR of ICAM-1 mRNA and the HuR translocation in HASMCs.

Reishi extract was chosen for testing, as it has long been known as a health food and used as traditional Chinese medicines. Its beneficial effects are thought to be due to its anti-inflammatory, antitumor, antioxidant, and immunomodulatory actions (*8*−*11*). A *Ganoderma* extract prevented albumin-induced oxidative damage of proximal tubular epithelial cells in an experimental setting, mimicking the proteinuric state (*21*), and reduced LPS-induced superoxide anion production by macrophages (*15*). *G. lucidum* polysaccharide-linked peptide reduced the production of the proinflammatory cytokines interleukin (IL-6) and monocyte chemoattractant protein (MCP-1) by activated rheumatoid synovial fibroblasts (*22*). Our previous report demonstrated an EORP-associated protective mechanism against bacteria infection involving enhancement of IL-1 expression and the clearance of LPS by macrophages (*23*). The present study is the first to report that EORP strongly reduces the expression of ICAM-1 mRNA and protein in any cell type, in this case LPS-treated HASMCs.

LPS treatment regulates ICAM-1 mRNA levels at the posttranscriptional level (*24*). Posttranscriptional regulation of ICAM-1 mRNA (stability, localization, and translation) is recognized as an important control point in ICAM-1 mRNA metabolism during inflammatory processes. AREs, located in the 3′-UTR of the mRNAs coding for certain cytokines, including ICAM-1 mRNA, are strong determinants of cytoplasmic mRNA turnover (*25*). HuR, an ubiquitous protein belonging to the embryonic lethal abnormal vision family of RNA-binding proteins, selectively binds to AREs and stabilizes ARE-containing mRNAs (*19*). LPS increases tumor necrosis factor-α expression in macrophages exposed to ethanol for 48 h, and RNA stabilization via the AREs in the 3′-UTR contributes to this increase (*26*). Our data show that HuR interacts directly with the 3′-UTR of ICAM-1 mRNA and that HuR is an essential regulator of ICAM-1 expression in LPS-stimulated HASMCs. In addition, EORP reduced LPS-induced ICAM-1 expression through posttranscriptional regulation, and this effect was mediated by inhibition of cytoplasmic shuttling of HuR.

The activation of various intracellular pathways by inflammatory stimuli, such as LPS, is required for the production of these adhesion molecules and proinflammatory chemokines (*20*). LPS-induced inflammatory responses, such as ICAM-1 expression in HASMCs, are regulated via toll-like receptor (TLR)4 expression (*27*). Most notably, the TLR4-mediated signaling pathway for LPS, leading to the activation of various intracellular kinases, including MAPKs and transcription factors, appears critical for the development of vascular inflammation and disease (*4*). Our study showed that LPS caused strong activation of three MAPK subtypes in HASMCs, as reported in a previous study (*28*).

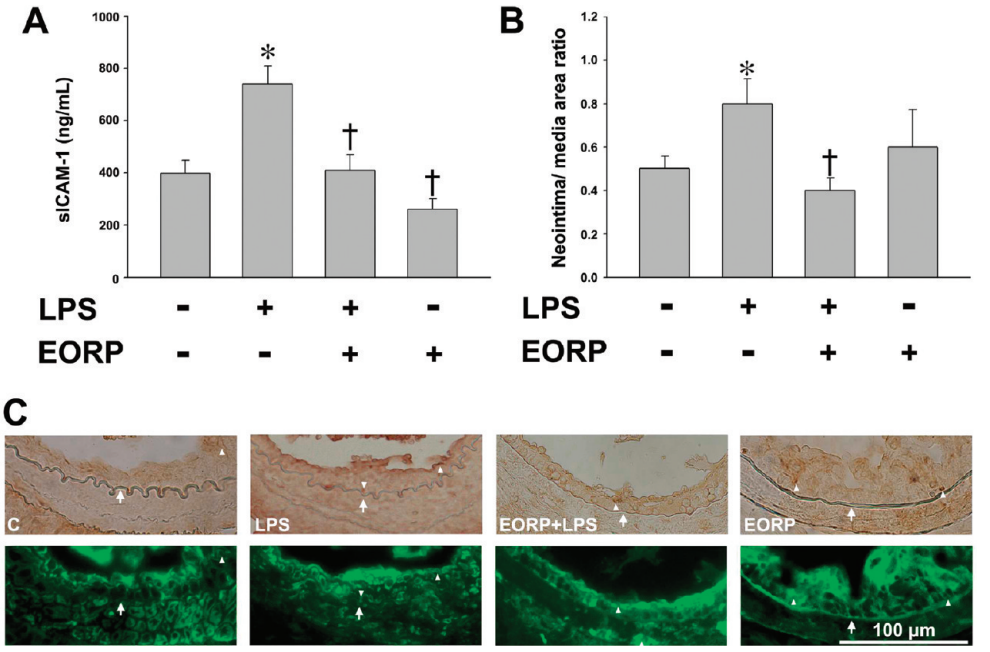

Figure 6. EORP decreases ICAM-1 expression in the LPS-treated endothelial-denuded artery in mice. (**A**) ICAM-1 concentration in the plasma analyzed by ELISA. $^{*}P < 0.05$ as compared to the unstimulated group. $^{\dagger}P < 0.05$ as compared to the LPS-treated group. (**B**) The mean of neointima/media area ratio of femoral arteries (**C**) Immunohistochemical staining for ICAM-1 (upper panels) and smooth muscle cells (lower panels) in serial sections of the femoral artery from LPS-treated endothelial-denuded mice. The lumen is uppermost in all sections. The internal elastic membrane is indicated by the arrow. The arrowhead indicates ICAM-1 positive overlapping with smooth muscle cell-specific staining. Bar = 50 μm $^{*}P < 0.05$ as compared to the unstimulated group. $^{\dagger}P < 0.05$ as compared to the LPS-treated group.

However, the involvement of their activation in the protective mechanism of EORP remains unclear. In the present study, the increase in ICAM-1 expression induced by LPS was markedly suppressed in the presence of an ERK inhibitor (PD98059) but not a p38 inhibitor (SB203580) or a JNK inhibitor (SP600125). ICAM-1 expression was also inhibited by ERK-specific siRNA. EORP decreased LPS-induced ERK phosphorylation. Thus, one of the mechanisms by which EORP reduces LPS-induced ICAM-1 expression involves a reduction in ERK1/2 activation. Consistent with our results, a *G. lucidum* extract inhibited the oxidative stress-induced phosphorylation of ERK1/2 in breast cancer cells, resulting in suppression of IL-8 secretion and finally in inhibition of cell migration (*29*). Another study showed that a *G. lucidum* extract inhibited prostate cancer-dependent angiogenesis by inhibition of phosphorylation of ERK1/2 and Akt kinases (*30*). In contrast, EORP induces IL-1 expression in macrophages and IL-2 expression in human T cells via the phosphorylation of MAPKs (*12*,*31*). The differences between the above results in terms of the pathways involved may be related to the different cell types used and the cytokines examined.

The binding of LPS to its receptor causes activation of two major transcriptional factors, NF-κB and AP-1, which, in turn, induce the expression of genes involved in chronic and acute inflammatory responses (*20*). NF-κB and AP-1 transcriptional activity can be modulated by the phosphorylation of MAPKs. These findings raised the possibility that EORP reduces ICAM-1 expression through a reduction in NF-κB activity. Our study demonstrated that the EORP-induced decrease in ICAM-1 expression was mediated through inactivation of NF-κB binding activity. Pretreatment with an NF-κB inhibitor also suppressed the LPS-induced increase in ICAM-1 expression, whereas an AP-1 inhibitor had no effect. This is consistent with a previous report that a *G. lucidum* extract inhibited the proliferation of human breast cancer cells by downregulation of NF-κB signaling (*32*). NF-κB is activated by signals possibly involving phosphorylation of the IκB subunit and its dissociation from the inactive cytoplasmic complex, followed by translocation of the active p50/p65 dimer to the nucleus (*33*). We demonstrated that the EORP-induced decrease in ICAM-1 expression was mediated through inhibition of p50 translocation.

It has been reported that administration of *G. lucidum* polysaccharides to normal fasted mice elicits hypoglycemia (*34*) and that a polysaccharide extract isolated from *G. lucidum* protects rat cerebral cortical neurons from hypoxia/reoxygenation injury (*35*). LPS-induced systemic inflammatory responses increase neointimal formation after balloon injury and stent implantation, and inflammatory cytokines are produced by VSMCs in the neointima (*36*). In the present study, EORP reduced monocyte−smooth muscle cell adhesion, and this effect was mediated through the decrease in ICAM-1 expression. In addition, EORP was shown to significantly reduce both the area of restenotic lesions and the ICAM-1 expression in the LPS-treated endothelial-denuded artery. On the basis of the probable involvement of ICAM-1 in monocyte recruitment to the neointima, our findings suggest an additional mechanism by which EORP treatment may be important in preventing the progression of cardiovascular disorders and inflammation.

In conclusion, this study provides the first evidence that EORP reduces ICAM-1 expression both in vitro and in vivo and also decreases leukocyte adhesion to HASMCs. The present data suggest that these effects might be mediated through inhibition of ERK phosphorylation and NF-κB activation. Because the recruitment of monocytes into the vascular wall after their adhesion to smooth muscle cells is a crucial step in the pathogenesis of vascular diseases, our study implies that EORP may have an, as yet, unexplored therapeutic potential in the prevention of cardiovascular disorders, with additional beneficial effects in multiple pathological events involving leukocyte adhesion, including inflammation and vascular diseases. The results of the present study suggest a possible therapeutic role for *G. lucidum* extract in cardiovascular disorders and in other inflammatory diseases.

LITERATURE CITED

(1) Ross, R. Atherosclerosis—An inflammatory disease. *N. Engl. J. Med.* **1999**, *340*, 115–126.

(2) Braun, M.; Pietsch, P.; Schrör, K.; Baumann, G.; Felix, S. B. Cellular adhesion molecules on vascular smooth muscle cells. *Cardiovasc. Res.* **1999**, *41*, 395–401.

(3) Collins, T.; Read, M. A.; Neish, A. S.; Whitley, M. Z.; Thanos, D.; Maniatis, T. Transcriptional regulation of endothelial cell adhesion molecules: NF-kappa B and cytokine-inducible enhancers. *FASEB J.* **1995**, *9*, 899–909.

(4) Muslin, A. J. MAPK signalling in cardiovascular health and disease: molecular mechanisms and therapeutic targets. *Clin. Sci.* **2008**, *115*, 203–218.

(5) Haverslag, R.; Pasterkamp, G.; Hoefer, I. E. Targeting adhesion molecules in cardiovascular disorders. Cardiovasc. *Hematol. Disord.: Drug Targets* **2008**, *8*, 252–260.

(6) Shiao, M. S. Natural products of the medicinal fungus *Ganoderma lucidum*: Occurrence, biological activities, and pharmacological functions. *Chem. Rec.* **2003**, *3*, 172–180.

(7) Wang, Y. Y.; Khoo, K. H.; Chen, S. T.; Lin, C. C.; Wong, C. H.; Lin, C. H. Studies on the immuno-modulating and antitumor activities of *Ganoderma lucidum* (Reishi) polysaccharides: Functional and proteomic analyses of a fucose-containing glycoprotein fraction responsible for the activities. *Bioorg. Med. Chem.* **2002**, *10*, 1057–1062.

(8) Gao, Y.; Gao, H.; Chan, E.; Tang, W.; Xu, A.; Yang, H.; Huang, M.; Lan, J.; Duan, W.; Xu, C.; Zhou, S. Antitumor activity and underlying mechanisms of ganopoly, the refined polysaccharides extracted from *Ganoderma lucidum*, in mice. *Immunol. Invest.* **2005**, *34*, 171–198.

(9) Miyazaki, T.; Nishijima, M. Studies on fungal polysaccharides. XXVII. Structural examination of a water-soluble, antitumor polysaccharide of *Ganoderma lucidum*. *Chem. Pharm. Bull.* **1981**, *29*, 3611–3616.

(10) Sun, J.; He, H.; Xie, B. J. Novel antioxidant peptides from fermented mushroom *Ganoderma lucidum*. *J. Agric. Food Chem.* **2004**, *52*, 6646–6652.

(11) Wang, S. Y.; Hsu, M. L.; Hsu, H. C.; Tzeng, C. H.; Lee, S. S.; Shiao, M. S.; Ho, C. K. The anti-tumor effect of *Ganoderma lucidum* is mediated by cytokines released from activated macrophages and T lymphocytes. *Int. J. Cancer* **1997**, *70*, 699–705.

(12) Hsu, H. Y.; Hua, K. F.; Lin, C. C.; Lin, C. H.; Hsu, J.; Wong, C. H. Extract of Reishi polysaccharides induces cytokine expression via TLR4-modulated protein kinase signaling pathways. *J. Immunol.* **2004**, *173*, 5989–5999.

(13) Lieu, C. W.; Lee, S. S.; Wang, S. Y. The effect of *Ganoderma lucidum* on induction of differentiation in leukemic U937 cells. *Anticancer Res.* **1992**, *12*, 1211–1215.

(14) Cao, L. Z.; Lin, Z. B. Regulation on maturation and function of dendritic cells by *Ganoderma lucidum* polysaccharides. *Immunol. Lett.* **2002**, *83*, 163–169.

(15) Woo, C. W. H.; Man, R. Y. K.; Siow, Y. L.; Choy, P. C.; Wan, E. W. Y.; Lau, C. S.; Karmin, O. *Ganoderma lucidum* inhibits inducible nitric oxide synthase expression in macrophages. *Mol. Cell. Biochem.* **2005**, *275*, 165–171.

(16) Jiang, J.; Slivova, V.; Valachovicova, T.; Harvey, K.; Sliva, D. *Ganoderma lucidum* inhibits proliferation and induces apoptosis in human prostate cancer cells PC-3. *Int. J. Oncol.* **2004**, *24*, 1093–1099.

(17) Lin, Y. L.; Liang, Y. C.; Lee, S. S.; Chiang, B. L. Polysaccharide purified from *Ganoderma lucidum* induced activation and maturation of human monocyte-derived dendritic cells by the NF-κB and p38 mitogen-activated protein kinase pathways. *J. Leukocyte Biol.* **2005**, *78*, 533–543.

(18) Sata, M.; Maejima, Y.; Adachi, F.; Fukino, K.; Saiura, A.; Sugiura, S.; Aoyagi, T.; Imai, Y.; Kurihara, H.; Kimura, K.; Omata, M.; Makuuchi, M.; Hirata, Y.; Nagai, R. A mouse model of vascular injury that induces rapid onset of medial cell apoptosis followed by reproducible neointimal hyperplasia. *J. Mol. Cell Cardiol.* **2000**, *32*, 2097–2104.

(19) Brennan, C. M.; Steitz, J. A. HuR and mRNA stability. *Cell. Mol. Life Sci.* **2001**, *58*, 266–277.

(20) Jersmann, H. P. A.; Hii, C. S. T.; Ferrante, J. V.; Ferrante, A. Bacterial lipopolysaccharide and tumor necrosis factor α synergistically increase expression of human endothelial adhesion molecules through activation of NF-κB and p38 mitogen-activated protein kinase signaling pathways. *Infect. Immun.* **2001**, *69*, 1273–1279.

(21) Lai, K. N.; Chan, L. Y. Y.; Tang, S. C. W.; Leung, J. C. K. Ganoderma extract prevents albumin-induced oxidative damage and chemokines synthesis in cultured human proximal tubular epithelial cells. *Nephrol., Dial., Transplant.* **2006**, *21*, 1188–1197.

(22) Ho, Y. W.; Yeung, J. S. L.; Chiu, P. K. Y.; Tang, W. M.; Lin, Z. B.; Man, R. Y. K.; Lau, C. S. *Ganoderma lucidum* polysaccharide peptide reduced the production of proinflammatory cytokines in activated rheumatoid synovial fibroblast. *Mol. Cell. Biochem.* **2007**, *301*, 173–179.

(23) Hua, K. F.; Hsu., H. Y.; Chao, L. K.; Chen, S. T.; Yang, W. B.; Hsu, J.; Wong, C. H. *Ganoderma lucidum* polysaccharides enhance CD14 endocytosis of LPS and promote TLR4 signal transduction of cytokine expression. *J. Cell. Physiol.* **2007**, *212*, 537–550.

(24) Wu, S. Q.; Aird, W. C. Thrombin, TNF-α, and LPS exert overlapping but nonidentical effects on gene expression in endothelial cells and vascular smooth muscle cells. *Am. J. Physiol. Heart Circ. Physiol.* **2005**, *289*, 873–885.

(25) Champelovier, P.; Pautre, V.; ElAtifi, M.; Dupré, I.; Rostaing, B.; Michoud, A.; Berger, F.; Seigneurin, D. Resistance to phorbol ester-induced differentiation in human myeloid leukemia cells: A hypothetic role for the mRNA stabilization process. *Leuk. Res.* **2006**, *30*, 1407–1416.

(26) McMullen, M. R.; Cocuzzi, E.; Hatzoglou, M.; Nagy, L. E. Chronic ethanol exposure increases the binding of HuR to the TNFα 3′-untranslated region in macrophages. *J. Biol. Chem.* **2003**, *278*, 38333–38341.

(27) Heo, S. K.; Yun, H. J.; Noh, E. K.; Park, W. H.; Park, S. D. LPS induces inflammatory responses in human aortic vascular smooth muscle cells via Toll-like receptor 4 expression and nitric oxide production. *Immunol. Lett.* **2008**, *120*, 57–64.

(28) Chen, Y. L.; Hu, C. S.; Lin, F. Y.; Chen, Y. H.; Sheu, L. M.; Ku, H. H.; Shiao, M. S.; Chen, J. W.; Lin, S. J. Salvianolic acid B attenuates cyclooxygenase-2 expression in vitro in LPS-treated human aortic smooth muscle cells and in vivo in the apolipoprotein-E-deficient mouse aorta. *J. Cell. Biochem.* **2006**, *98*, 618–631.

(29) Thyagarajan, A.; Jiang, J.; Hopf, A.; Adamec, J.; Sliva, D. Inhibition of oxidative stress-induced invasiveness of cancer cells by *Ganoderma lucidum* is mediated through the suppression of interleukin-8 secretion. *Int. J. Mol. Med.* **2006**, *18*, 657–664.

(30) Stanley, G.; Harvey, K.; Slivova, V.; Jiang, J.; Sliva, D. *Ganoderma lucidum* suppresses angiogenesis through the inhibition of secretion of VEGF and TGF-β1 from prostate cancer cells. *Biochem. Biophys. Res. Commun.* **2005**, *330*, 46–52.

(31) Hsu, H. Y.; Hua, K. F.; Wu, W. C.; Hsu, J.; Weng, S. T.; Lin, T. l.; Lin, C. Y.; Liu, C. Y.; Hseu, R. S.; Huang, C. T. Reishi immunomodulation protein induces interleukin-2 expression via protein kinase-dependent signaling pathways within human T cells. *J. Cell. Physiol.* **2008**, *215*, 15–26.

(32) Jiang, J.; Slivova, V.; Sliva, D. *Ganoderma lucidum* inhibits proliferation of human breast cancer cells by down-regulation of estrogen receptor and NF-κB signaling. *Int. J. Oncol.* **2006**, *29*, 695–703.

(33) Ghosh, S.; Baltimore, D. Activation in vitro of NF-kappa B by phosphorylation of its inhibitor I kappa B. *Nature* **1990**, *344*, 678–682.

(34) Zhang, H. N.; Lin, Z. B. Hypoglycemic effect of *Ganoderma lucidum* polysaccharides. *Acta Pharmacol. Sin.* **2004**, *25*, 191–195.

(35) Zhao, H. B.; Lin, S. Q.; Liu, J. H.; Lin, Z. B. Polysaccharide extract isolated from *Ganoderma lucidum* protects rat cerebral cortical neurons from hypoxia/reoxygenation injury. *J. Pharmacol. Sci.* **2004**, *95*, 294–298.

(36) Danenberg, H. D.; Welt, F. G. P.; Walker, M., III; Seifert, P.; Toegel, G. S.; Edelman, E. R. Systemic inflammation induced by lipopolysaccharide increases neointimal formation after balloon and stent injury in rabbits. *Circulation* **2002**, *105*, 2917–2922.

Received for review February 9, 2010. Revised manuscript received June 10, 2010. Accepted July 25, 2010. This work was supported by research grants from the National Science Council (NSC 96-2328-B-002-051-MY3 and NSC 95-2752-B-006-005-PAE) and the Cooperative Research Program of the NTU and CMUCM, Taiwan, Republic of China.